

# Site Dependency of Shallow Seismic Data Quality in Saturated, Unconsolidated Coastal Sediments

Jeffrey G. Paine, Robert A. Morton, and L. Edwin Garner

Bureau of Economic Geology  
The University of Texas at Austin  
University Station, Box X  
Austin, TX 78713, U.S.A.

## ABSTRACT

PAINE, J.G.; MORTON, R.A., and GARNER, L.E., 1997. Site Dependency of Shallow Seismic Data Quality in Saturated, Unconsolidated Coastal Sediments. *Journal of Coastal Research*, 13(2), 564-574. Fort Lauderdale (Florida), ISSN 0749-0208.



Seismic tests were conducted along the southeastern Texas coast to (1) investigate the usefulness of land-based shallow seismic reflection profiling, (2) examine the influence of environment on data quality, (3) evaluate compressional-wave sources for shallow profiling of unconsolidated sediments, and (4) determine the exploration depth range of shallow seismic reflection methods. Tests in three environments, including unvegetated beach, densely vegetated marsh, and densely vegetated floodplain, show that near-surface sediment characteristics strongly influence data quality. A modified soil probe hammer, which is a low-energy, broad-frequency-range seismic source, was used for the short reflection profiles at each site. Highest quality data were collected at the beach, where reflections were recorded as shallow as 7 m and as deep as 200 m. At the marsh and floodplain sites, surface wave velocities were higher, peak frequencies were lower, and exploration depths were limited. Despite similar target depths and near-surface water tables at each site, optimum acquisition parameters varied. Effects of extraneous noise associated with ambient conditions (wind, breaking waves, road traffic) were minimized with filters. Shallow seismic reflection methods can be applied to a variety of coastal geological and environmental problems including high-resolution studies of Quaternary strata, location of active near-surface faults, and delineation of buried archeological sites. On-land seismic surveys can also augment borehole data, guide borehole placement, and extend offshore surveys across the shoreline and onto the coastal plain.

**ADDITIONAL INDEX WORDS:** *Shallow seismic reflection profiling, Texas coastal plain, Quaternary.*

## INTRODUCTION

High-resolution seismic tests were conducted along the southeastern Texas coast at three sites between Galveston Bay and Sabine Pass (Figure 1). These tests were designed to investigate the usefulness of land-based seismic reflection profiling of Pleistocene and Holocene strata in representative coastal environments, examine the dependence of data quality on ground characteristics, evaluate compressional-wave seismic sources for ultra-shallow reflection profiling, and determine the effective depth range of low-energy seismic-reflection methods in these environments.

These three sites were selected because they represent different modern depositional environments and because moderately deep (10 to 30 m) hollow-stem auger cores drilled by the Bureau of Economic Geology were available from each site. The High Island site (Figure 1) is an interfluvial setting located between the partly drowned, incised valleys that form Galveston Bay and Sabine Lake. Seismic tests at High Island were completed on the barren, modern sandy beach near the high tide line. A core from a nearby borehole drilled on the beach to a depth of 10 m shows that the shallow strata consist of three units. A 1.5-m-thick veneer of Holocene sand and shelly sand (beach and washover deposits) overlies Holocene

marsh mud which extends to a depth of at least 4 m. The marsh mud, in turn, overlies upward-fining cycles of interbedded sand and mud interpreted as upper Pleistocene fluvial and deltaic deposits of the Beaumont Formation (BERNARD and LEBLANC, 1965; ARONOW and BARNES, 1982). The depth of the Holocene-Pleistocene unconformity at this location, which is between 4 and 5.5 m, is uncertain because both deposits are composed of mud.

The Sabine Pass site, located 4 km north of Sabine Pass (Figure 1), is in a topographically low, densely vegetated muddy marsh located between higher and sandier Holocene beach ridge deposits (GOULD and MCFARLAN, 1959). In two cores located southeast and northwest of the test site, the interpreted erosional Holocene-Pleistocene unconformity deepens from 8 m to 26 m into an incised valley that was a tributary to the ancestral Sabine River. Near-surface sediments (upper 6 to 8 m) are shelly sand and sandy mud deposited in Holocene marsh and beach ridge and swale environments. A thick section (6 to 26 m depth) of estuarine and deltaic muds (valley-fill deposits) underlies chenier plain deposits in the northwestern core.

Seismic tests also were conducted on the densely vegetated floodplain within the modern Neches River valley (FISHER *et al.*, 1973) along a bridge 2 km upstream from Sabine Lake (Figure 1). Core samples and foundation boring descriptions

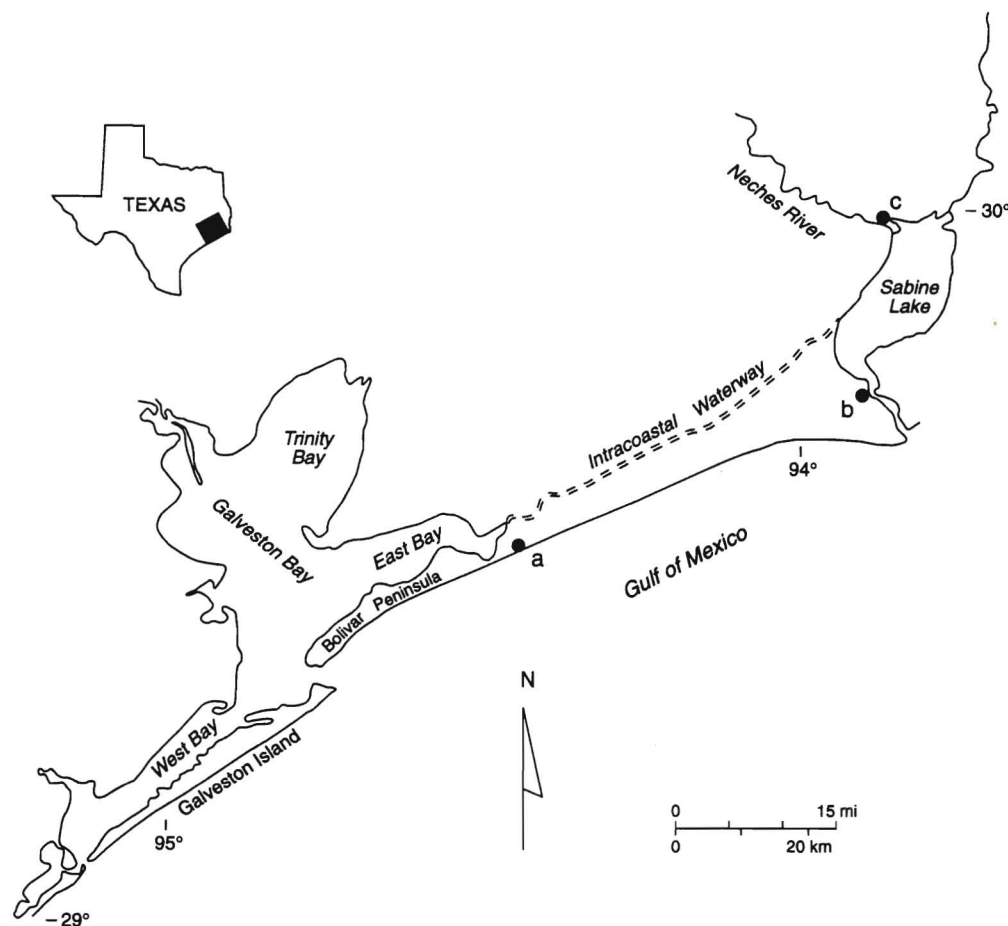


Figure 1. Map of the southeastern Texas coast showing the location of three seismic testing sites: (a) Gulf beach at High Island, (b) chenier plain marsh at Sabine Pass, and (c) modern floodplain along the Neches River.

from as deep as 35 m indicate that soft, organic-rich, clayey sediments, probably deposited in an aggrading floodplain environment, are present to a depth of about 10 m at the test site. These floodplain deposits are underlain by fine to medium sand interpreted to be fluvial deposits that may be stratigraphically equivalent to upper Pleistocene or lower Holocene Deweyville beds (BERNARD, 1950; BLUM *et al.*, 1995) exposed farther up the Neches River valley (SHELBY *et al.*, 1992). Below 17 m are stiff clay and sandy clay interpreted as upper Pleistocene fluvial and deltaic deposits of the Beaumont Formation.

Table 1. Equipment used to collect shallow seismic data at High Island, Sabine Pass, and Neches River test sites.

Energy sources	3.6 kg modified soil probe hammer (reflection source) 5.4 kg sledge hammer on aluminum plate (refraction source)
Geophones	Mark Products L-40A (40 Hz, 515 ohm coil resistance, 13 cm spikes)
Seismograph	Bison 9048 (48 channel, 16 bit analog to digital conversion)

## METHODS

### Seismic Tests

Seismic tests performed at each site included noise, filter, and source tests that were used to optimize acquisition geometry and recording settings for short reflection surveys. For these tests, the seismograph was connected to a linear array of 48 high-frequency geophones spaced at 1-m intervals (Tables 1 and 2). For the noise test, the seismograph recorded background seismic noise with no source activated. This test and observations made during the surveys revealed that important sources of noise were wind (at each site), breaking waves (at the High Island site), vehicle noise (at the Sabine Pass and Neches River sites), and bridge vibrations (at the Neches River site). Wind noise was largely unavoidable, as was constant vehicle noise at the bridge over the Neches River. Noise from breaking waves and bridge vibrations was reduced by using low-cut filters during data acquisition, and vehicle noise was avoided at the Sabine Pass site by recording only when no vehicles were near the site.

Filter tests were conducted to determine the optimum set-

Table 2. Recording parameters and acquisition geometry used during seismic reflection surveys.

	High Island	Sabine Pass	Neches River
Spread type	End-on	End-on	Split
Source to near-trace offset (m):	1	1	1
Spread length (m)	47	47	23
Source stacks	1	1	1
Geophones in array	1	1	1
Geophone spacing (m)	1	1	1
Recording channels	48	48	48
Sample interval (s)	0.001	0.0005	0.0005
Record length (s)	1.0	0.25	0.25
Analog low-cut filter (Hz)	16	32	64
Analog high-cut filter (Hz)	1,000	1,000	1,000
Data fold	24	48	24

ting for the analog low-cut filter. The intent was to raise the filter as high as possible to reduce low-frequency surface wave noise, but keep it low enough to allow a wide-frequency range and to allow the deepest events of interest to be recorded. Tests using the chosen acquisition geometry and low-cut filter settings of 4, 8, 16, 32, 64, 96, 128, and 192 Hz showed that the optimum filter setting was 16 Hz for the High Island site, 32 Hz for the Sabine Pass site, and 64 Hz for the Neches River site (Table 2).

Compressional wave sources available for the field tests included a sledgehammer and a modified soil probe hammer (Table 1). The sledgehammer was struck on an aluminum plate resting on the ground. The soil probe hammer, originally manufactured to collect small diameter soil cores, consists of a sliding 3.6 kg weight mounted on a metal rod. The weight is driven downward by hand over a 45 cm stroke and strikes the top of a rod. A 225-cm<sup>2</sup> steel plate welded to the base of the rod delivers the seismic energy to the ground. This source produces less seismic energy than does the sledgehammer but is easy to use and provides a consistent seismic pulse. Electronic switches mounted to the sources provided time breaks for the seismograph.

Stacking tests were conducted using the source-receiver geometry selected for the reflection lines. The soil probe hammer was fired repeatedly into the geophone spread in an attempt to increase the signal-to-noise ratio by partly canceling random noise. One shot per shotpoint was chosen to keep possible minor discrepancies in shot times from degrading the high-frequency part of the source spectrum.

Other acquisition parameters selected on the basis of these tests included a seismograph sampling interval of 0.0005 to 0.001 s and a record length of 0.25 to 1 s (Table 2). A Global Positioning System receiver accurate to 1 m was used to locate end points of the surveys.

### Acquisition Geometry

A short seismic-reflection line was acquired at each of the three sites using the common-depth-point method adapted to shallow subsurface surveys (MAYNE, 1962; MILLER *et al.*, 1990; STEEPLES and MILLER, 1990). Because we were interested in imaging the shallowest reflections possible, the min-

imum source-receiver distance was 1 m (Table 2). The farthest offset generally should be equal to or greater than the depth of the deepest target. Using 1-m shotpoint and geophone spacing, the maximum source-receiver offset was 24 m at the Neches River site and 48 m at the High Island and Sabine Pass sites (Table 2). Source-receiver geometries were symmetric (split spread geometry with 24 geophones on each side of the shotpoint) at the Neches River site and were asymmetric (end-on geometry with the source trailing the geophone spread) at the High Island and Sabine Pass sites. One 40-Hz geophone was used at each geophone location for each line.

### Data Processing

Seismic data were processed using the software SPW on a Macintosh computer and employing procedures common to many types of reflection processing (YILMAZ, 1987). The first processing step was to convert the data files to SPW format. Next, trace headers were created that combined the seismic data with acquisition-geometry information. Dead or excessively noisy traces were then deleted from the data set. Automatic gain control was applied to amplify weak arrivals at late times or far offsets. A mute function was designed to delete the first arrivals from each shot gather to prevent them from stacking as a false reflector. Another mute function was designed to remove the air wave, or the sound of the source traveling through the air, from each shot gather. Bandpass filtering removed unwanted low- and high-frequency noise from the Sabine Pass and Neches River data sets. Velocity analysis was conducted by fitting reflection hyperbolas to events on common midpoint (CMP) gathers (all traces that have the same source-receiver midpoint, but different offsets). For 24-fold data, there are 24 traces in a CMP gather.

The velocity function derived from the CMP gathers was used to correct each trace in the gather for normal moveout (the delay in arrival time caused by increasing source-receiver offset) and to simulate zero offset for all traces. Each velocity-corrected trace in a CMP gather was summed to produce a single composite trace. A stacked seismic section is a display of these composite traces.

## RESULTS

### Gulf Beach at High Island

The highest quality seismic data from all three sites were recorded at High Island (Figure 1) along a line oriented parallel to the shoreline. This orientation is approximately parallel to depositional strike of the coastal-plain deposits. A sample field record from the short reflection survey at this site (Figure 2), recorded with one shot from the soil probe hammer and a 16-Hz low-cut filter, shows several types of seismic energy. Visible phases (Figure 2a) include (1) high-amplitude, low-frequency, and slowly propagating surface waves (lower left of field record, less than 80 m/sec propagation velocity), (2) an air wave, or the sound of the hammer blow traveling in air (high frequency, 330 m/sec propagation velocity), (3) a critically refracted arrival from the near-sur-

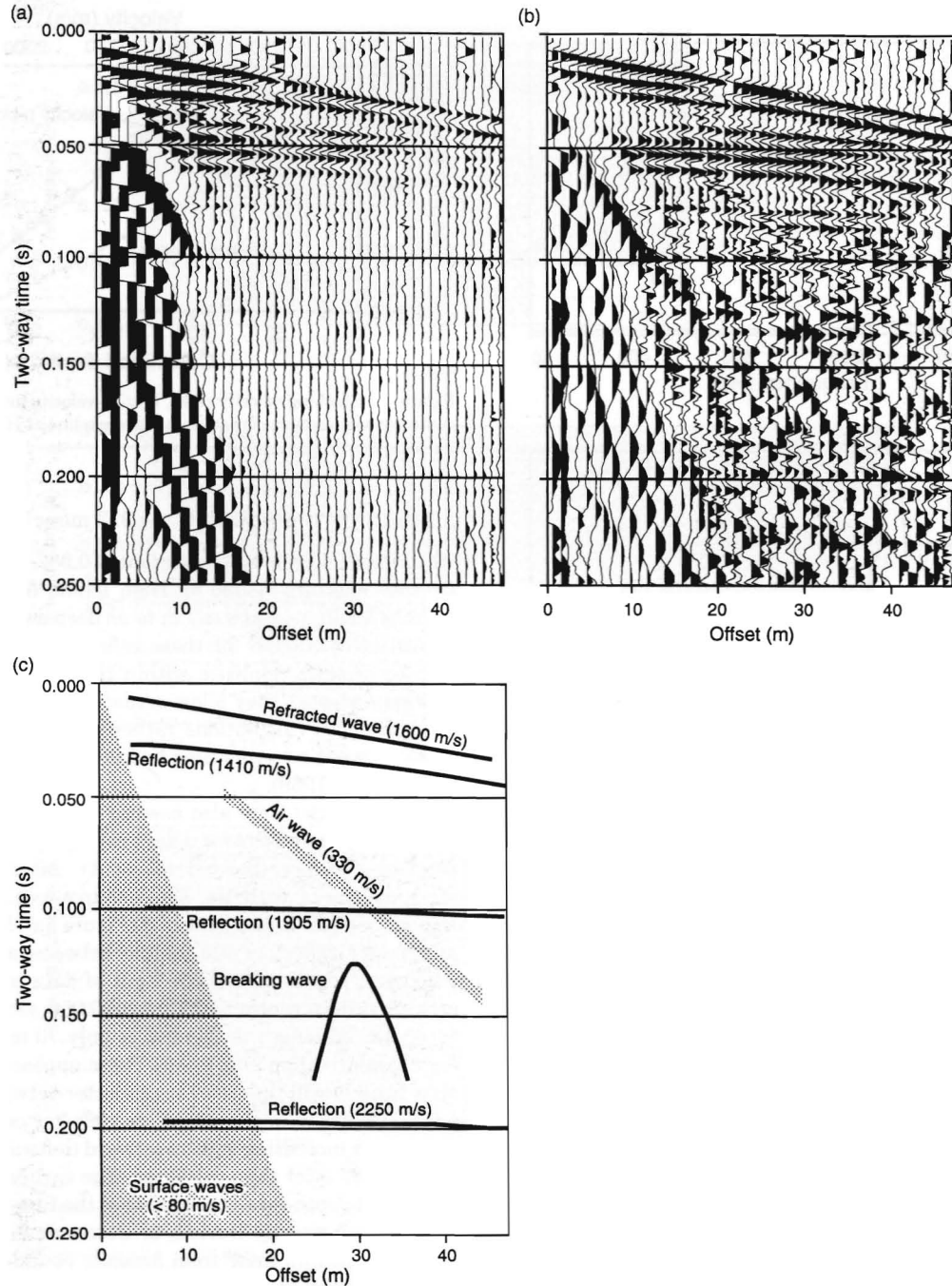


Figure 2. (a) Field record from High Island with 36 dB display gain, (b) field record with automatic gain control (0.05 s window) applied, and (c) interpreted types of seismic energy.

face water table (1600 m/sec propagation velocity), and (4) a few hyperbolic reflectors between 0 and 0.080 s two-way time. With automatic gain control applied (Figure 2b), later reflectors are visible (to 0.200 sec). Also visible at about 30 m offset is the hyperbolic signature of an oceanic wave breaking on the shoreface of the Gulf of Mexico.

The strongest events on these field records are the low-

frequency surface waves (Figures 2, 3a), which commonly obscure shallow reflectors in reflection surveys. At High Island, near-surface compressional velocities are about 20 times higher than surface wave propagation velocities (Figure 2c). This allows early reflections (0.010 sec and later) to arrive at the geophones before the surface waves at near-source distances. Power spectra of individual traces at High Island

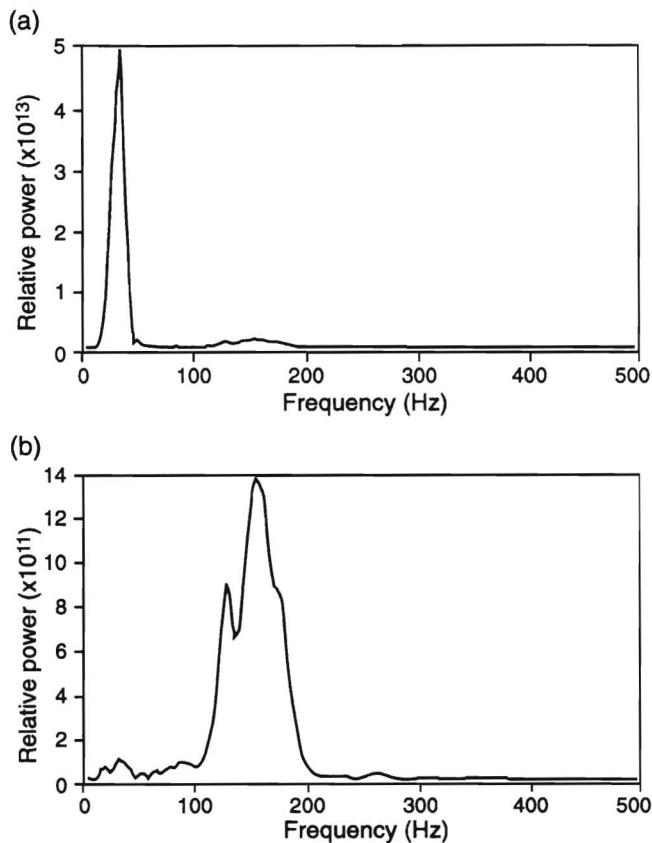


Figure 3. High Island power spectrum at 10 m source-receiver offset, (a) before and (b) after surface wave mute.

show a power peak at about 30 Hz and a secondary peak at about 150 Hz (Figure 3a). After muting the surface-wave-dominated part of the field record, the remainder of the seismic energy on the 10 m trace is mostly reflected and refracted energy and has a band of significant power between 100 and 200 Hz and a peak at about 150 Hz (Figure 3b). This peak is one to two orders of magnitude weaker than that for the surface waves.

Compressional wave velocities picked for hyperbolic reflectors visible on CMP gathers show that velocities increase with two-way time (Figure 4). Velocities increase rapidly from about 1300 m/sec to 1500 m/sec between 0.020 and 0.050 sec, then increase more slowly to about 2250 m/sec at 0.200 sec. Increased velocities at depth are related to physical properties of the sediments and geologic history of the area. Surficial and near-surface Holocene sediments tend to be soft with high water contents because they were deposited during the post-glacial rise in sea level and submergence of the coastal plain. In contrast, deeper strata are more compacted because they were subaerially exposed during the Wisconsin lowstands in sea level.

A best-fit velocity function calculated from least-squares regression of two-way times and stacking velocities can be used to convert time to depth for the seismic data (Figure 4). This function is

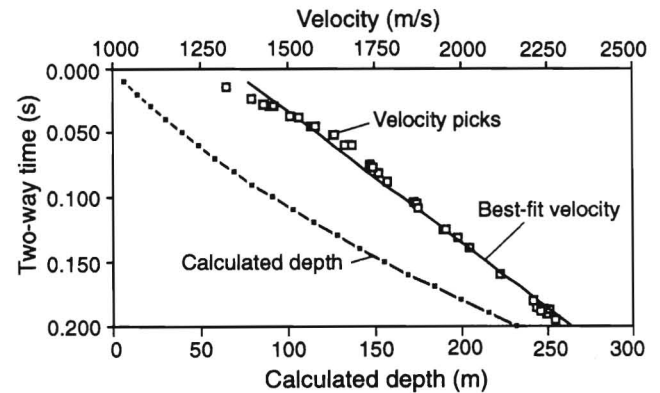


Figure 4. Stacking velocity picks, best-fit velocity function, and time-to-depth conversion curve for seismic reflection line at High Island test site.

$$\text{velocity} = \text{two-way time} \times 4,913 \text{ m/sec}^2 + 1,337 \text{ m/sec},$$

which has a correlation coefficient of 0.987. Calculated depths for the reflectors visible on High Island field records range from as shallow as about 7 m to as deep as 200 m (Figure 4). Velocities calculated for these reflectors yield new information on seismic velocities within the upper Pleistocene and Holocene strata. They allow actual measured velocities to be used in depth calculations rather than theoretical relationships between two-way time and depth, such as the one used by LEHNER (1969).

Velocity picks were also used to correct traces of different source-receiver offsets for delays caused by increasing source-receiver distance (normal moveout). After correcting and stacking traces with the same source-receiver midpoint, a seismic section was constructed (Figure 5a). Numerous major and minor reflectors are visible between about 0.010 and 0.250 sec, which include the limit of data processed. Strong seismic reflectors are visible near 0.050 sec, 0.125 sec, and 0.180 sec. Although the section is only 70 m long, some geological information is present. There appears to be a narrow structural low in the 0.020 sec reflector between CMP 32 and 38, a broad low in the 0.060 sec reflector centered on CMP 30, and an increasing southwestward (leftward) apparent dip of reflectors later than 0.100 sec. The earliest reflector has a calculated depth that is near that of the Pleistocene-Holocene contact in a nearby Bureau of Economic Geology borehole. Deeper reflectors arise from acoustic boundaries within upper Pleistocene and older strata.

### Marsh at Sabine Pass

At the chenier plain marsh, source and noise tests were performed first and then shallow reflection data (Table 2) were obtained along a short line oriented approximately perpendicular to the shoreline (depositional dip). Data were acquired employing one soil probe hammer pulse at each shotpoint in an end-on configuration in both line directions that resulted in 96 traces per shotpoint. A relative amplitude display of a typical field record, in which the highest recorded amplitudes are equalized among the traces, reveals that low-

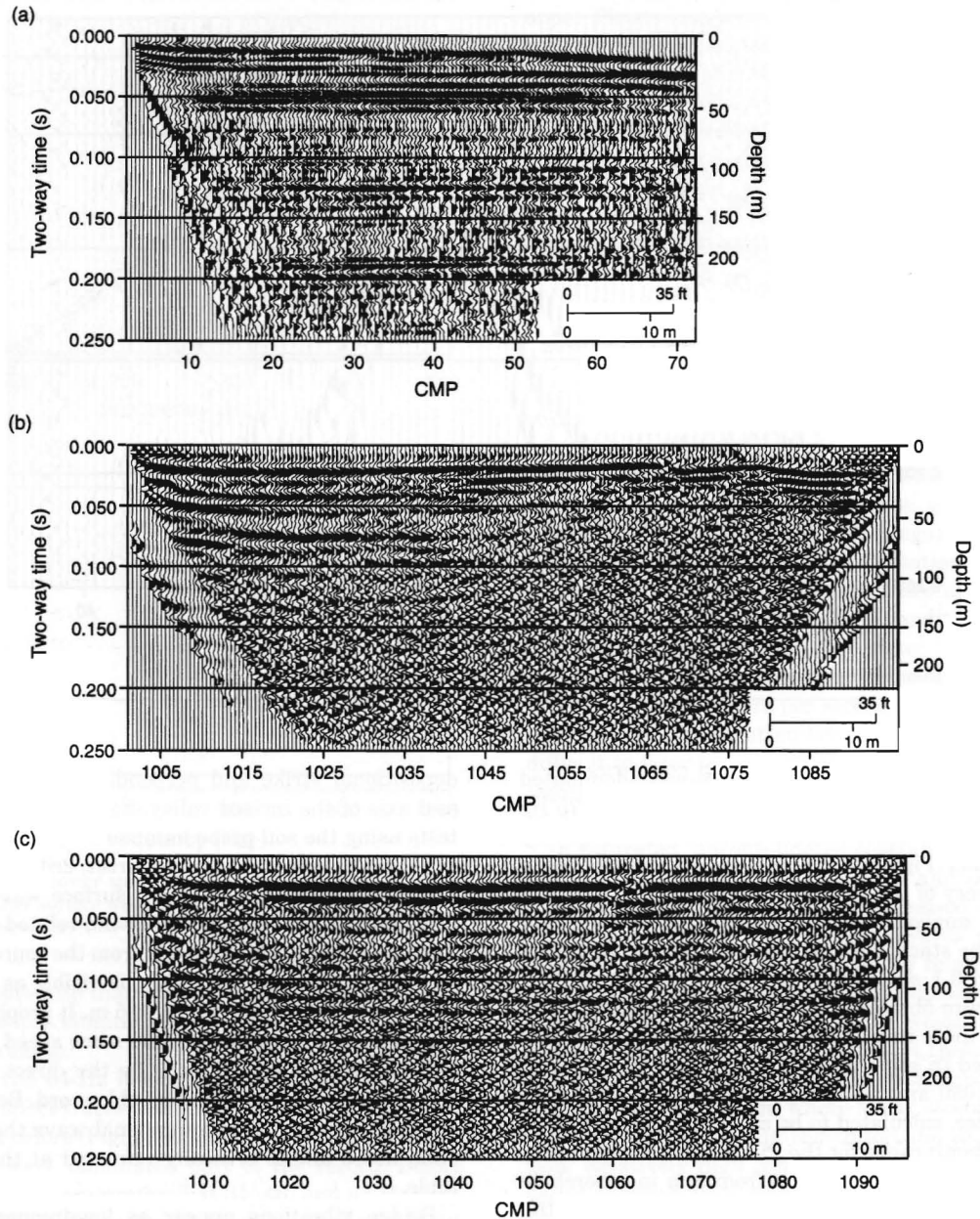


Figure 5. Processed seismic reflection sections from test sites at (a) High Island, (b) Sabine Pass, and (c) Neches River. Traces are 0.5 m apart and are displayed with automatic gain control (0.1 s window) applied.

frequency surface waves, high-frequency air waves, and random noise are all clearly recorded at the site (Figure 6). A few reflection hyperbolas are also visible, particularly at about 0.025 sec, between 0.040 and 0.050 sec, and at about 0.080 sec. Other reflectors are either not present or are obscured by strong surface waves or noise. Data quality deteriorates with increasing offset, and reflectors are difficult to see on the field record beyond about 35 m.

The propagation velocity of the surface waves is as high as 150 m/sec, nearly twice as high as that at the High Island site. These faster surface waves increase the offset distance

by which there is adequate separation between the arrival times of the reflected energy and the surface waves, which in turn increases the minimum exploration depth. Using a near-surface velocity of 1400 m/sec and a zero offset two-way time of the earliest observed reflection of 0.020 sec, the shallowest visible reflector corresponds to a depth of 14 m. The deepest reflector visible on the field record arrives at about 0.130 sec, which corresponds to a depth of about 120 m.

A power spectrum calculated for a trace with a 10 m source-receiver separation shows that most of the recorded seismic signal is below 100 Hz (Figure 7a). Power peaks at

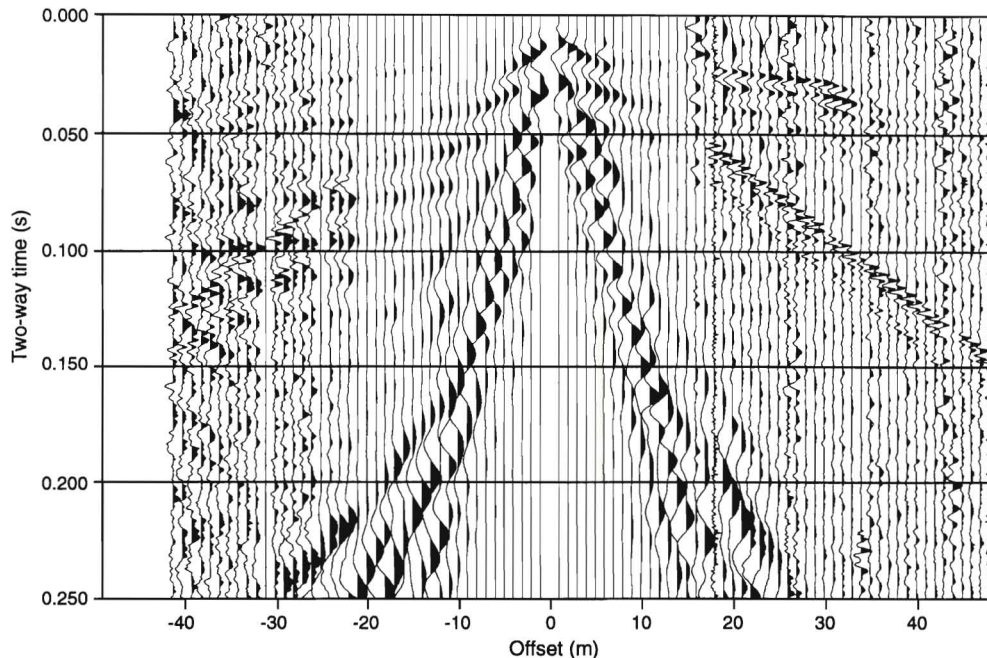


Figure 6. Field record from Sabine Pass site. Highest amplitudes in each trace have been equalized.

30 and 50 Hz are removed when the surface-wave-dominated part of the shot record is muted, and are replaced by a 70 Hz peak that is about 15 times weaker than the low-frequency surface wave peaks (Figure 7b). This probably represents the dominant frequency of the reflected energy.

After velocity analysis, normal moveout correction, and CMP stacking, the stacked section shows a few strong reflectors earlier than 0.1 sec and a few weaker reflectors later than 0.1 sec (Figure 5b). Reflection peaks are broader (lower frequency) than those in the High Island section and reflections are obscured in some parts of the Sabine Pass section (between CMP 1050 and 1075, for example). The strong reflector at 0.020 sec, calculated to be at a depth of 14 m, falls in the expected depth range for the Pleistocene-Holocene erosional contact. This contact deepens from 8 m in a borehole southeast of the site to 26 m in a borehole northwest of the site. Earlier arrivals in the stacked section may represent a weak reflection off the interface between chenier plain deposits and underlying bay and bayhead delta muds.

In general, the Sabine Pass section has a lower signal-to-noise ratio than the High Island section. Because much of the noise appears to be random wind-related noise and because there is little significant transmitted energy above 100 Hz, the signal-to-noise ratio might be improved in similar environments by stacking several shots at each shotpoint.

### Neches River Floodplain

At the Neches River site, seismic tests and a short reflection survey were completed on the vegetated floodplain in the right-of-way of a heavily trafficked bridge crossing the Neches River. The seismic line at this site was aligned parallel to

depositional strike and perpendicular to the modern river and axis of the incised valley. Field records of low-cut filter tests using the soil probe hammer source show several types of recorded energy, including direct, critically refracted, and reflected compressional waves, surface waves, an air wave, bridge vibrations, and random wind-related noise (Figure 8). The direct wave, which travels from the source to the receiver without appreciable refraction, is visible as the first arrival at source-receiver offsets of 1 to 5 m. It propagates across the spread at 333 m/sec, nearly the same speed as the air wave, and is distinguished from it by the direct wave's leftward (downward) deflection on the field record. Beyond 5 m offset, the first arrival is a compressional wave that propagates at 1565 m/sec and is critically refracted at the shallow water table.

Bridge vibrations appear as low-frequency, high-amplitude, leftward-propagating waves on the field records (Figure 8a, b). With a dominant frequency of about 16 Hz, this noise source is diminished by applying a 16 Hz low-cut filter (Figure 8b) and almost completely removed by applying a 64 Hz filter (Figure 8c). Surface waves are also a low-frequency noise source that propagate at about 100 m/sec at the Neches River site. The effect of increasing the low-cut filter is to remove progressively more of the low-frequency-dominated surface waves. Surface wave strength is noticeably diminished as the filter was raised from 16 Hz to 64 Hz and finally 96 Hz (Figures 8b, c, and d). Along with the desirable reduction in surface wave strength is a reduction in reflected energy strength, which produces an undesirable decrease in signal-to-noise ratio, particularly at the 96 Hz low-cut filter setting (Figure 8d). A setting of 64 Hz was chosen for the reflection

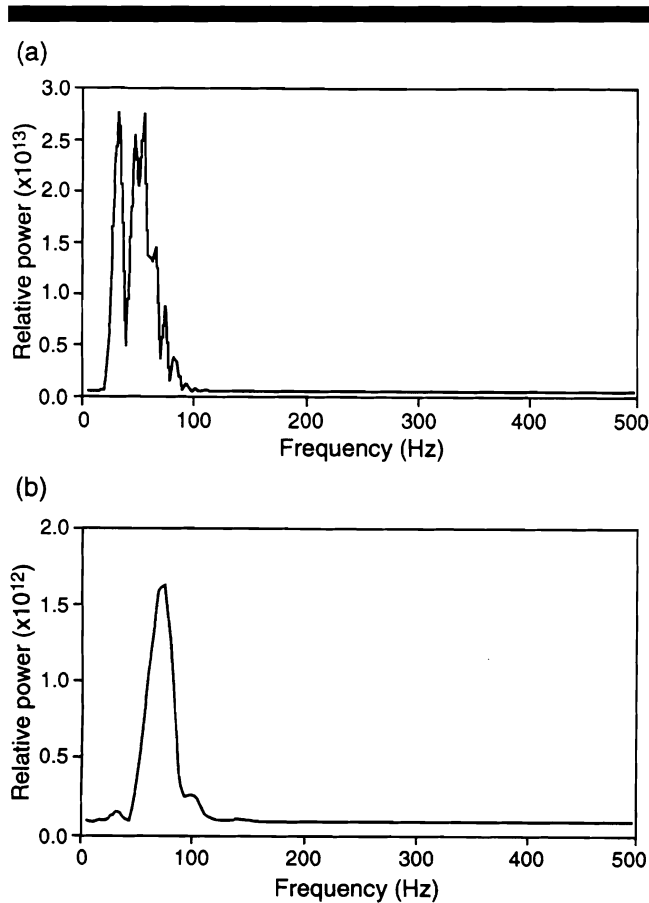


Figure 7. Sabine Pass power spectrum at 10 m source-receiver offset, (a) before and (b) after surface wave mute.

survey as a compromise that allowed enough reflected signal to be recorded while eliminating bridge noise and reducing surface wave strength.

The effect of the 64-Hz low-cut filter is shown on power spectra of 10-m offset traces from the Neches River reflection survey, recorded before (Figure 9a) and after (Figure 9b) muting the surface-wave dominated part of the record. Before muting, power peaks are centered at 31, 46, and 63 Hz (Figure 9a). After muting the surface-wave dominated part of the record, the 31 Hz and 46 Hz peaks are diminished and the 63 Hz peak remains nearly as strong as it was before the mute (Figure 9b). Unlike surveys at High Island and Sabine Pass, where lower low-cut filters were employed, the low-frequency (less than 50 Hz) surface wave peaks are weaker at the Neches River site than the recorded compressional wave signal. Like at the Sabine Pass marsh site, little seismic energy above 100 Hz was recorded.

Processing steps to produce a stacked section (Figure 5c) included surface wave, air wave, and first-arrival mutes, bandpass filtering, velocity analysis, moveout correction, and CMP stacking. A weak reflector appears to be present as early as 0.015 sec, which corresponds to a depth of about 8 m. This horizon may be an inadvertent stack of a weak refracted arrival, or it may correlate to the stratigraphic boundary be-

tween muddy Holocene floodplain deposits and underlying upper Pleistocene or lower Holocene Deweyville sands penetrated in nearby cores and foundation borings. A stronger reflector arrives at 0.025 sec two-way time, which converts to 18 m depth. This is near the 17 m depth at which stiff upper Pleistocene clay and sandy clay of the Beaumont Formation are found in the borings. Several reflectors are visible as late as 0.130 sec, which corresponds to a depth of 120 m. Overall data quality is better than that at the Sabine Pass marsh and not as good as that at the High Island beach.

## DISCUSSION

### Surface Wave and Compressional Wave Separation

A major limitation of compressional wave reflection surveys of the shallow subsurface is the interference of surface waves and reflected waves at near-source distances. Because the vertical component of surface waves is much stronger than that of typical reflected waves, geophone response is dominated by surface wave motion regardless of the dynamic range of the seismograph. This limitation is particularly severe where near-surface sediments are dry (air-filled pores) and unconsolidated. Under these conditions, compressional velocities can be less than 1000 m/sec (PAINE, 1994), which are not much greater than typical surface wave velocities of several hundred meters per second. Also, higher seismic frequencies are rapidly attenuated in dry sediments, making it difficult to filter low-frequency surface waves without significantly degrading the overlapping frequency range of the reflected waves.

In saturated, unconsolidated coastal sediments, which are represented by the three test sites and common in many parts of the world, adequate separation between surface waves and reflected compressional waves is attained much closer to the sound source due to the relatively low surface-wave velocities (80 to 150 m/sec at the coastal sites) and relatively high compressional wave velocities (about 1500 m/sec). Low surface wave velocities at these sites are caused by the low shear strength of the coastal deposits and are lowest for the sandy beach, where shear strength is further reduced by lack of binding vegetation and sediment consolidation. Relatively high compressional wave velocities are the result of water-filled rather than air-filled pores. At High Island, for example, reflectors at two-way times as early as 0.010 sec were recorded. While this is an early time, relatively high compressional velocities also mean that (1) the earliest observable reflector may be deeper than the near-surface zone of interest, and (2) seismic wavelengths are longer for a given frequency than in environments with lower compressional velocities, which reduces vertical resolution proportionately.

High-resolution seismic surveys involving shear waves offer promise if shallower target depths are desired than those practical for compressional-wave surveys. Shear-wave surveys take advantage of lower velocities to increase resolution and use horizontally polarized shear waves to reduce the strength of the recorded surface wave. In areas with low shear strength such as the barren beach, however, it may be difficult to generate recordable shear waves.

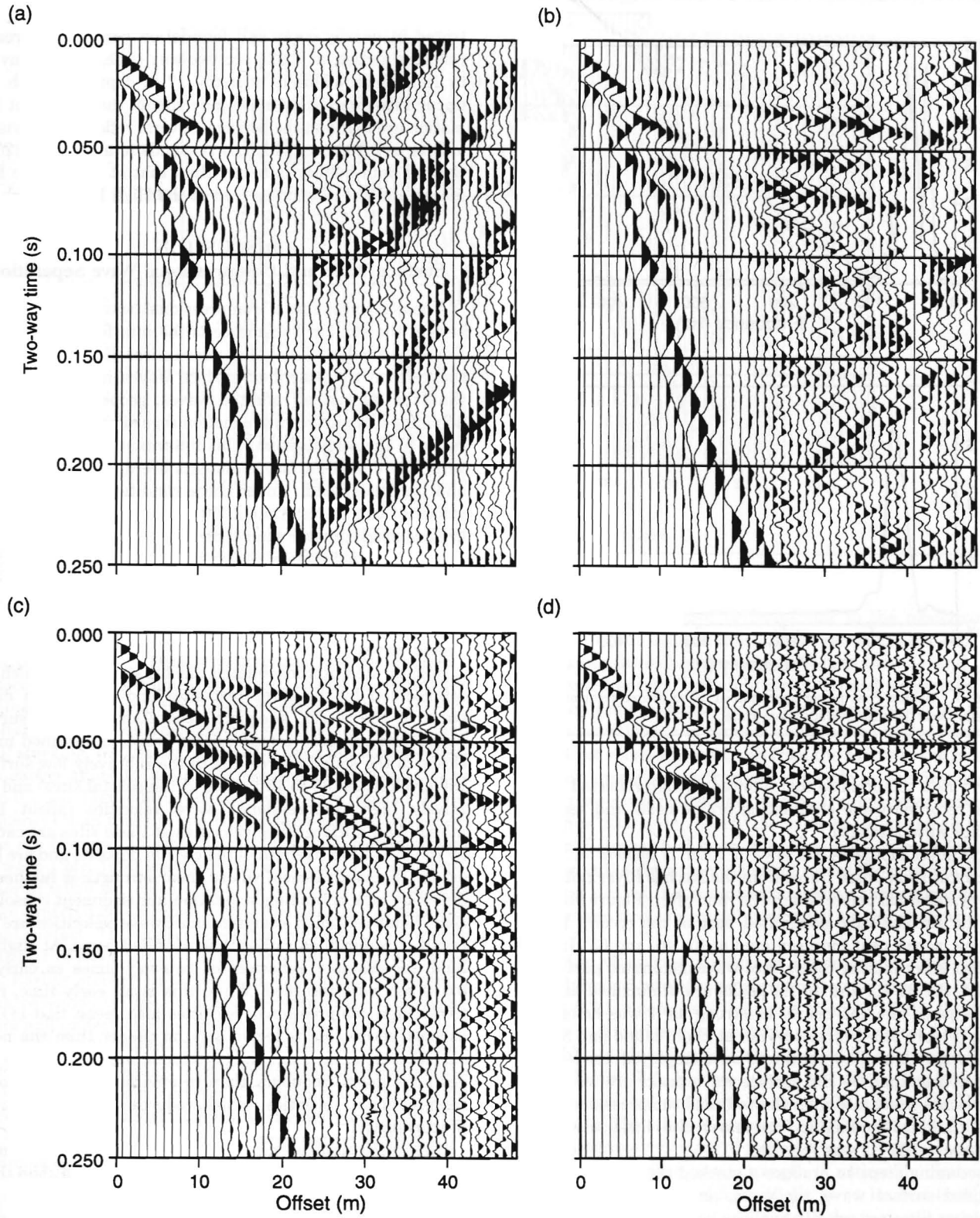


Figure 8. Field records from low-cut filter test at Neches River site. During the test, data were acquired with the low-cut filter at (a) 4 Hz, (b) 16 Hz, (c) 64 Hz, and (d) 96 Hz. Records displayed with highest amplitude equalized for each trace.

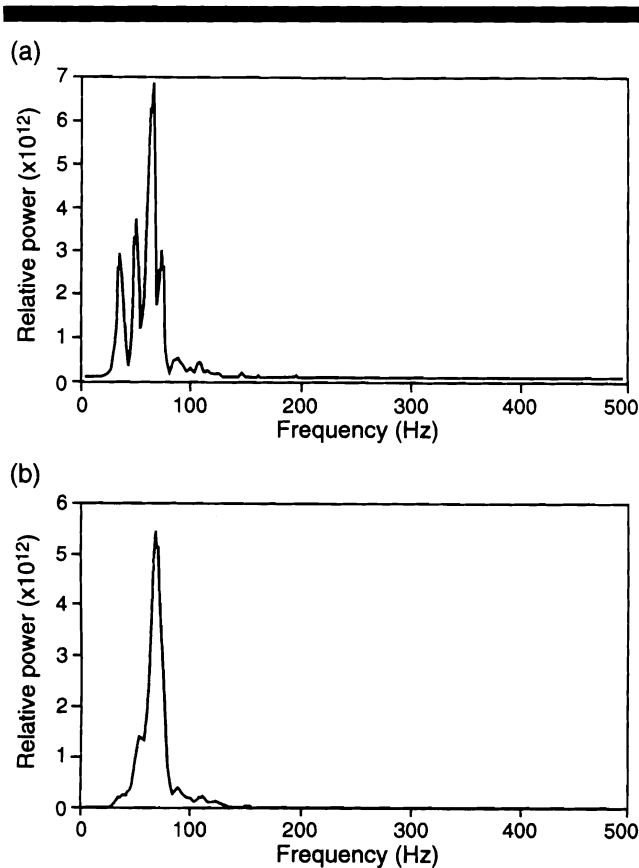


Figure 9. Neches River power spectrum at 10 m source-receiver offset, (a) before and (b) after surface wave mute.

### Frequency Ranges

Frequency ranges are important for seismic profiling because broader frequency ranges and higher frequencies increase seismic resolution and make it easier to filter surface wave noise. One issue is the frequency range of the source pulse, and another is the frequency range of the reflected wave at the geophone after subsurface attenuation. Hammer sources such as those used at the three coastal sites are considered to be low-frequency sources compared to explosive and projectile sources (MILLER *et al.*, 1986). Power spectra calculated after surface wave mutes show the highest frequency range at the High Island site, where peak signal power was recorded between 100 and 200 Hz. This implies that the soil probe hammer source produces significant seismic energy at least as high as 200 Hz. At seismic velocities of 1500 m/sec, the wavelength at 200 Hz is 7.5 m. The theoretical limit of vertical resolution is between 1/4 and 1/8 wavelength (WIDESS, 1973), which is between 1 and 2 m.

Frequency range and vertical resolution are not as favorable at the Sabine Pass marsh and the Neches River floodplain. After surface wave mutes, peak seismic energy is found between 50 and 90 Hz at Sabine Pass and between 55 and 80 Hz at the Neches River. The same source was used at all three sites and there was little difference in coupling between

the source and the land surface. Lower frequencies recorded at the Sabine Pass and Neches River sites are likely due to preferential subsurface attenuation of higher frequencies. The limit of vertical resolution at these sites is 2 to 4 m.

### Exploration Depths

Determining both the minimum and maximum exploration depth was an objective of this study, but the minimum depth was more critical because the geological targets were within the Holocene and late Pleistocene units near the surface. For compressional wave surveys, minimum exploration depth depends primarily on the velocity difference between surface waves and compressional waves, which was greatest at High Island. At this site, the earliest reflector visible over an adequate range of source-receiver offsets arrived at about 0.010 sec, which corresponds to a depth of about 7 m. This is at or below the contact between Holocene and Pleistocene sediments, thus only reflectors within Pleistocene strata are visible on the reflection line. The Sabine Pass and Neches River sites have similar near-surface compressional wave velocities but higher surface wave velocities, which suggests that earliest detectable reflectors are later than 0.010 sec and deeper than 7 m. The shallowest visible reflectors are calculated at 14 m for Sabine Pass and 8 m at the Neches River. Because both sites overlie former incised valleys, the minimum depths of visible reflectors are sufficiently shallow to image some Holocene deposits.

Maximum exploration depths are greater than expected given the small size and low energy of the sound source. Reflections were recorded as late as 0.200 sec at High Island and 0.130 sec at the Sabine Pass and Neches River sites. Velocity analysis at these relatively late times is hindered by the acquisition geometry designed for shallower reflectors, but estimated depths to the deepest reflectors are 200 m at High Island and about 120 m at the Sabine Pass and Neches River sites.

### Potential Applications

Seismic reflection methods adapted for the shallow subsurface have several potential applications in coastal environments such as those represented along the southeastern Texas coast. Seismic tests carried out in this study demonstrate that reflection surveys can allow a better understanding of Holocene and upper Pleistocene strata as shallow as a few meters below the land surface. Reflection surveys can provide a geological context for existing boreholes, both between and beneath the holes, and can guide placement of new boreholes. They can augment an abundance of existing high-resolution inner shelf and estuarine seismic reflection data with needed shallow data landward of the shoreline. Finally, reflection surveys such as those carried out in this study can be used to determine offset on numerous reactivated coastal zone faults such as those mapped by WHITE and TREMBLAY (1995).

### CONCLUSIONS

Shallow seismic reflection profiling using small impulsive sources is a viable method of imaging near-surface Holocene

and upper Pleistocene strata along the southeastern Texas coast. The modified soil probe hammer is a simple, low-energy, broad-frequency-range seismic source that generates a consistent seismic pulse with frequencies to at least 200 Hz. It has a practical exploration depth range of 5 to more than 100 m at these coastal sites. Tests at three representative coastal environments, including unvegetated beach, densely vegetated marsh, and densely vegetated floodplain, show that near-surface sediment characteristics strongly influence data quality. Highest quality data were collected from the sandy beach environment, where surface-wave velocities were below 80 m/sec, recorded peak frequencies were between 100 to 200 Hz, and reflections were recorded as shallow as 7 m and as deep as 200 m. Data quality in the muddy marsh at Sabine Pass and the vegetated muddy floodplain along the Neches River was not as good. At these sites, surface wave velocities were higher, peak frequencies were below 100 Hz, minimum exploration depths were deeper (8 to 10 m), and maximum exploration depths were shallower (about 120 m). Shallower exploration depths might be achieved using seismic techniques that employ shear-wave sources.

Despite similar target depths and near-surface water tables at each test site, optimum acquisition parameters, processing steps, and processing parameters differed. Effects of extraneous noise associated with ambient conditions (wind, breaking waves, road traffic) were eliminated or minimized with filters. On the beach, where the only major noise sources were wind and breaking waves, one shot per shotpoint and a relatively low filter setting of 16 Hz produced good data. In the marsh, where data quality was poor perhaps because of trapped organic gases in pore space, a low-cut filter setting of 32 Hz diminished surface wave noise. More shots at each shotpoint might reduce random wind-related noise at this site. At the floodplain site, where data quality was moderate, a high filter setting of 64 Hz was required to diminish traffic noise, source-related surface waves, and bridge vibrations.

Similar shallow reflection surveys are relatively easy to perform and may prove useful in a variety of coastal environments. Potential applications of this technique include studies of Quaternary strata, near-surface faulting, and buried archeological sites. On-land surveys can augment borehole data, guide placement of boreholes, and extend offshore and estuarine seismic surveys across the critical land-sea boundary.

#### ACKNOWLEDGEMENTS

This study was partly supported by the U.S. Geological Survey, Coastal Geology Program under grant 14-08-0001-

A0912. Publication was authorized by the Director, Bureau of Economic Geology, The University of Texas at Austin.

#### LITERATURE CITED

- ARONOW, SAUL and BARNES, V.E., 1982. *Geologic Atlas of Texas, Houston sheet*. The University of Texas at Austin, Bureau of Economic Geology, map scale 1:250,000.
- BERNARD, H.A., 1950. *Quaternary Geology of southeast Texas*. Baton Rouge, Louisiana, Louisiana State University, Ph.D. thesis, 164p.
- BERNARD, H.A. and LEBLANC, R.J., 1965. Résumé of the Quaternary geology of the northwestern Gulf of Mexico province, In: WRIGHT, H.E., JR. and FREY, D.G. (eds.), *The Quaternary of the United States*. Princeton, New Jersey: Princeton University Press, pp. 137-185.
- BLUM, M.D.; MORTON, R.A., and DURBIN, J.E., 1995. "Deweyville" terraces and deposits of the Texas Gulf Coastal Plain: A reevaluation. *Transactions Gulf Coast Association of Geological Societies*, 45, 53-60.
- FISHER, W.L.; BROWN, L.F., JR.; MCGOWEN, J.H., and GROAT, C.G., 1973. *Environmental geologic atlas of the Texas coastal zone, Beaumont-Port Arthur area*: The University of Texas at Austin, Bureau of Economic Geology, 93p.
- GOULD, H.R. and MCFARLAN, E., 1959. Geologic history of the chenier plain southwestern Louisiana. *Transactions Gulf Coast Association of Geological Societies*, 9, 261-270.
- LEHNER, P., 1969. Salt tectonics and Pleistocene stratigraphy on continental slope of northern Gulf of Mexico. *American Association of Petroleum Geologists Bulletin*, 53, 2431-2479.
- MAYNE, W.H., 1962. Common reflection point horizontal data stacking techniques. *Geophysics*, 27, 927-938.
- MILLER, R.D.; PULLAN, S.E.; WALDNER, J.S., and HAENI, F.P., 1986. Field comparison of shallow seismic sources. *Geophysics*, 51, 2067-2092.
- MILLER, R.D.; STEEPLES, D.W.; HILL, R.W., JR., and GADDIS, B.L., 1990. Identifying intra-alluvial and bedrock structures shallower than 30 meters using seismic reflection techniques, In: WARD, S.H. (ed.), *Geotechnical and environmental geophysics*. Society of Exploration Geophysicists, *Investigations in Geophysics No. 5*, 3, 89-97.
- PAINE, J.G., 1994. Subsidence beneath a playa basin on the Southern High Plains, U.S.A.: evidence from shallow seismic data. *Geological Society of America Bulletin*, 106, 233-242.
- SHELBY, C.A., PIEPER, M.K., ARONOW, S., and BARNES, V.E., 1992. *Geologic Atlas of Texas, Beaumont sheet*. The University of Texas at Austin, Bureau of Economic Geology, map scale 1:250,000.
- STEEPLES, D.W. and MILLER, R.D., 1990. Seismic reflection methods applied to engineering, environmental, and groundwater problems, In: S.H. WARD, (ed.), *Geotechnical and environmental geophysics*, Society of Exploration Geophysicists, *Investigations in Geophysics No. 5*, 1, 1-30.
- WHITE, W.A. and TREMBLAY, T.A., 1995. Submergence of wetlands as a result of human-induced subsidence and faulting along the upper Texas Gulf Coast. *Journal of Coastal Research*, 11, 788-807.
- WIDESS, M.B., 1973. How thin is a thin bed? *Geophysics*, 38, 1176-1180.
- YILMAZ, O., 1987. Seismic data processing. Society of Exploration Geophysicists, *Investigations in Geophysics No. 2*, 526p.